

ARMScope – THE VERSATILE PLATFORM FOR SCANNING PROBE MICROSCOPY SYSTEMS

Bartosz Świadkowski, Tomasz Piasecki, Maciej Rudek, Michał Świątkowski, Krzysztof Gajewski, Wojciech Majstrzyk, Michał Babij, Andrzej Dzierka, Teodor Gotszalk

Wrocław University of Science and Technology, Faculty of Microsystem Electronics and Photonics, Janiszewskiego 11-17, 50-372 Wrocław, Poland (✉ bartosz.swiadkowski@pwr.edu.pl, +48 71 320 3202, tomasz.piasecki@pwr.edu.pl, maciej.rudek@pwr.edu.pl, michal.swiatkowski@pwr.edu.pl, krzysztof.gajewski@pwr.edu.pl, wojciech.majstrzyk@pwr.edu.pl, michal.babij@pwr.edu.pl, adzierka@gmail.com, teodor.gotszalk@pwr.edu.pl)

Abstract

Scanning probe microscopy (SPM) since its invention in the 80's became very popular in examination of many different sample parameters, both in university and industry. This was the effect of bringing this technology closer to the operator. Although the ease of use opened a possibility for measurements without high labour requirement, a quantitative analysis is still a limitation in Scanning Probe Microscopes available on the market. Based on experience of Nano-metrology Group, SPM still can be considered as a tool for quantitative examination of thermal, electrical and mechanical surface parameters.

In this work we present an ARMScope platform as a versatile SPM controller that is proved to be useful in a variety of applications: from atomic-resolution STM (*Scanning Tunnelling Microscopy*) to Multi-resonance KPFM (*Kelvin Probe force microscopy*) to commercial SEMs (*Scanning electron microscopes*).

Keywords: Scanning probe microscopy, AFM, Kelvin Probe force microscopy, scanning tunnelling microscopy.

© 2020 Polish Academy of Sciences. All rights reserved

1. Introduction

Scanning probe microscopy (SPM) belongs to the technologies enabling to examine electrical, thermal, optical and mechanical surface parameters. The basic idea of the SPM technology is to observe the so-called near-field interactions between the tip and the sample. SPM techniques have evolved significantly since their invention in the 80's improving their capabilities and introducing new measurement modes [1]. In the last three decades SPM has become very popular in the university and industrial laboratories, mostly because of an enormous progress making this technology more user/operator-friendly and more reliable. Progress in the SPM technology can be identified in many fields.

Mechanical SPM heads are manufactured as rigid and compact components enabling high speed surface scanning and immunity against vibration. Optical detectors of the tip displacement are designed as compact units making adjustments easier and more stable [2]. Also, resolution of the probe deflection in a range of tens of $\text{fm/Hz}^{1/2}$ was presented [3].

The sample scanning is controlled by piezo-actuators integrated with external measurement units determining the actuator position [4, 5]. The actuator resonance frequencies are increasing and thus making the video surface scanning possible [6–8]. In the SPM examinations a variety of cantilevers integrated with various tips can be applied. They exhibit rigidity and changing resonance frequency in a range from 0.1 N/m up to 100 N/m and from 5 kHz up to 1 MHz, respectively. Tips of various shapes, including *e.g.* super sharp, high aspect ratio, sphere probes and tailored to chemical and/or physical properties can be applied in the sample examinations. In this way not only the surface topography is recorded but its chemical and physical properties as well. The SPM applications span from microbiology and biotechnology up to material science and micro- and nano-electronics [9–12].

Despite enormous progress in this field several limitations of the SPM technology must be identified as well. Difficulties in the metrology (in other words in the quantitative analysis) of the recorded phenomena and limited throughput of the surface analysis belong to the most important ones. In many publications the SPM metrology is associated with the so-called dimensional metrology but, based on the experience of the Nanometrology Division, the SPM techniques can be applied in the quantitative examinations of thermal, electrical and mechanical surface parameters.

However, in this case the development of new scanning, control, data acquisition and signal processing schemes is almost always necessary. There are SPM systems available on the market, which are mostly optimized from the utilitarian point of view and are usually used as closed systems. Their architecture provides the researcher with little space for the system modification and its adaptation to the experimental requirements. In general, two classes of the microscope setups can be distinguished. The first is the hardware-oriented one, which means that a variety of system components can be applied to construct an instrument. However, in this case the possibilities of implementing novel control and measurement algorithms are limited [13]. The second class is the software-oriented one, which describes systems whose hardware environment is defined [14]. They offer some flexibility which is however influenced by the hardware components. Additionally, the information describing the controller setup is usually supplied to promote the product from the marketing point of view and contains too little metrological data.

In our solution we are able to configure the hardware components in an arbitrary way and have the full access to the software making it possible to define any control and measurement algorithm. It consists of three main functional blocks. The first one is a measurement head equipped with a probe assembly, a piezoelectric scanner with a sample holder and a micro-cantilever deflection detector (for AFM mode) or a tunnelling current detector (for STM mode). The SPM head is fixed on the vibration damping setup and enclosed in a noiseless chamber.

The second part is a modular ARMScope SPM controller. Its brain is a system controller containing an embedded microprocessor (ARM7-based) whose firmware controls the measurement and data acquisition processes. It communicates with exchangeable modules such as: *analogue-to-digital converter* (ADC) module, *proportional – integral – derivative* (PID) controllers, a scan field controller or a stepper motor driver, by means of a dedicated system bus.

The third part is a user interface. The system controller communicates with the operator's workstation which is a typical personal computer at which the user uses a dedicated ARMScope application to control the measurement process. A general view of the system's components is shown in Fig. 1.

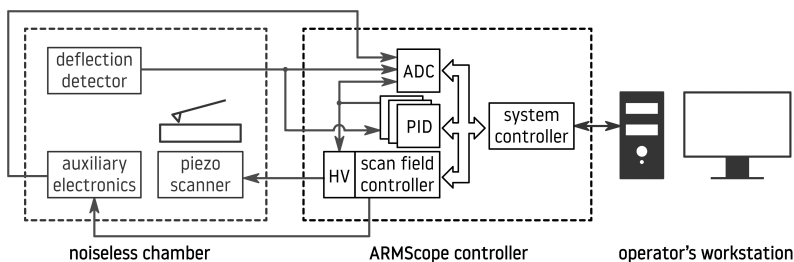


Fig. 1. A block diagram of ARMScope home-made scanning probe.

In this paper we present a so-called ARMScope platform, which makes it possible to perform metrological examinations of material and device nanostructure properties. The ARMScope applications span over standard topography measurements, multi-resonance *Kelvin Probe force microscopy* (KPFM) [15], thermal examinations in the so-called *load force modulation* (LoFM) [14] and *scanning tunnelling microscopy* (STM) [17]. Various types of the tip-surface interaction detectors have been applied in our experiments, which include *optical beam deflection* (OBD) detectors [15], piezo-resistive cantilevers [16] and electro-magnetic cantilevers [18]. The core of the system is the ARMScope controller, whose open and precisely defined architecture enables to adapt the system to measurements performed at the atomic or hundreds of micrometre scale with a scanning speed ranging from several to tens of lines per second. The architecture of the ARMScope controller will be discussed in detail, especially the methodology of characterization of the modules influencing the scanning and data acquisition process. These are the features of greatest importance for the development and application of the ARMScope controller in the metrological surface examinations.

2. ARMScope controller

2.1. System controller

In response to various needs of scanning probe microscopy, Nanometrology Division, Faculty of Microsystem Electronics and Photonics, Wrocław University of Science and Technology, fabricated and tested a universal microscope controller, adjustable to different kinds of examination, called ARMScope. During the design process, special attention was paid to modularity of both measurement electronics and control software. Specific functions were spread across easily interchangeable extension cards communicating with ARM (*Advanced RISC Machine*) MCU via *External Memory Interface* (EMI). Modularity of the applied solution enables to use as many cards for control and signal acquisition as necessary to perform specific measurements. The embedded software has a modular structure that increases its portability to novel hardware solutions. The implemented functional blocks reduce the cost of extending its functionality. The system controller is significantly supported by a home-made ARMSscanner software and embedded software kit controlling the ARM microprocessor. The software architecture is based on a common command pattern. Separated parts of the system communicate with ARM MCU using a defined set of commands. As a result of user actions, a related set of commands is created in the user interface (ARMSscanner). Using a dedicated transmission protocol, the settings are transmitted via USB interface. The protocol block of the system controller's firmware is responsible for decoding and analysing (*e.g.* verifying its correctness) incoming data frames. Depending on the

command type, the interrelated block of the controller is initialized and configured. The scanning process requires simultaneous signal generation and sampling. These functions are divided in two independent software blocks. The time-control block uses high-resolution hardware timers to provide necessary synchronization between other software modules. The block's behaviour is set with respect to the user-defined data that determine the positioning signal shape, timing, as well as sampling type. When all blocks are set, the execution module can be triggered which starts the whole process.

The PC software is the interface between the user and the MCU, enabling to change the measurement modes as well as their parameters. It is also responsible for the analysis of the results providing an online preview and correction of the measured sample property. Among ARMScanner's up-to-date features the most important are: supporting multiple measurement modes including sine and vector scanning, online image processing with a built-in module, error detection, multithreading and a very convenient and precise positioning system with intelligent navigation. In the vector scanning mode, which is one of the ARMScanner's newest features, the probe is moved according to any user-created pattern. Because of that, the overall path of the tip is shorter and the scan can be faster.

The main part of ARMScope SPM controller is an LPC 2478 MCU (Microcontroller Unit) that coordinates operation of the whole system using a 16-bit parallel bus and provides communication with PC. Every SPM needs common basic functions, like scanning field control, data acquisition and probe positioning, but there are also more advanced functions dedicated to a specific kind of measurement.

ARMScope scanner versatility was proved in various applications in Nanometrology Division laboratories. It is used as a controller of STM and AFM microscopes and was successfully applied to acquire images from vulnerable SEM microscopes: Hitachi S-570 and Jeol JSM-35.

2.2. Scan field controller

ARMScope controller is equipped with a dedicated Scan Field Controller. It consists of six DACs in total and an analogue section for scaling and rotation, which is a combination of digitally controlled potentiometers and adders. Its schematic is shown in Fig. 2. Its role is to convert the space of image coordinates into the space of sample coordinates (Fig. 2 – right) as:

$$x_s = x_0 + k \times \cos(\alpha) \times x - k \times \sin(\alpha) \times y, \quad (1)$$

$$y_s = y_0 + k \times \sin(\alpha) \times x + k \times \cos(\alpha) \times y, \quad (2)$$

where x_s, y_s are the coordinates in the sample space, x, y are the coordinates in the image space, k is a scaling factor, x_0, y_0 are offsets in the space of sample coordinates and α is the rotation

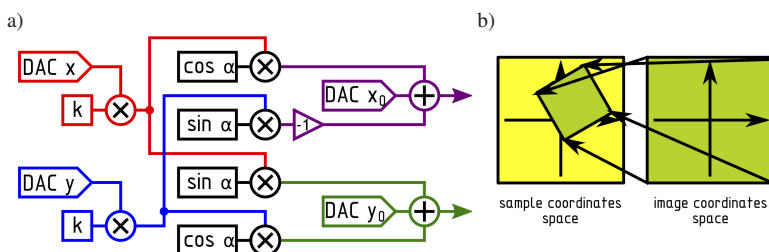


Fig. 2. A block diagram of the rotation and scaling section of the Scan field controller module (left) and a visualisation of sample transformation to the space of image coordinates (right).

angle. Thanks to the analogue rotation and scaling section, the system ensures the capacity of easy sample imaging manipulation without any loss in resolution and noise performance.

Our module, except for a classic raster scanning mode, provides a sine scan mode. In this pattern, the fast scan axis is driven by means of a sine signal, leading to a smoother piezoelectric scanner movement. This occurs due to the fact that the sine signal contains significantly fewer higher harmonic frequencies, compared with the triangle signal, which may cause piezoelectric element mechanical resonance during fast STM scans. The *Total Harmonic Distortion* (THD) parameter may be used to precisely define the number of harmonic components. Our system generates less than 0.5% THD during the sine scan mode with a speed of up to 10 lps compared with 12.1% THD of the triangle signal. By characterizing the piezoelectric scanner and comparing the results with the Scan Field Controller output spectrum it is possible to estimate and avoid the risk of introducing mechanical resonances of piezo-element. The spectra of the generated sine and triangle signals compared to the measured frequency response of our AFM piezoelectric scanner are shown in Fig. 3. The spectra were measured in the operating conditions, *i.e.* with a piezoelectric scanner mounted in AFM head with HOPG sample (sample weight 230 mg). The sine scan mode spectrum contains fewer and lower frequency peaks within a 100 kHz range, which results in a decreased deflection noise, as well as the possibility of piezoelectric resonance during the operation.

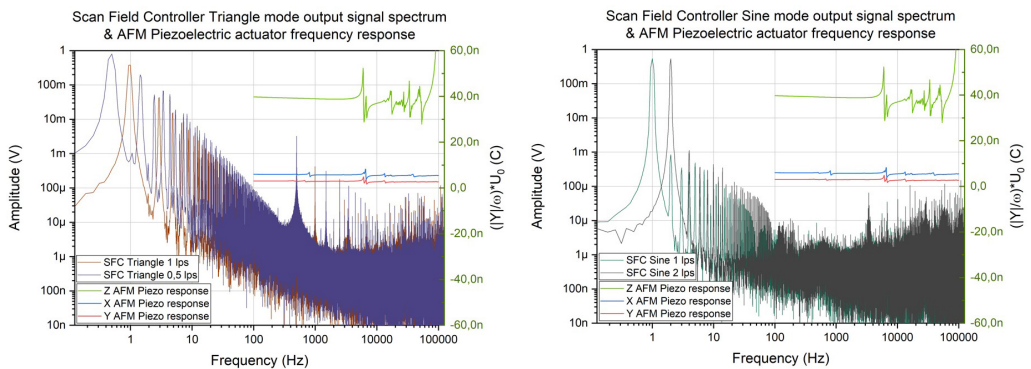


Fig. 3. The Scan Field Controller performance compared to the piezoelectric scanner frequency response: the AFM scanner and triangle scan mode (left), the AFM scanner and sine scan mode (right).

The resonances of the piezoelectric actuator may be easily detected using the *impedance spectroscopy* (IS). The IS is a method in which the impedance (or admittance) of a device under test is measured over a wide range of frequencies. One of the most common measurement techniques used in IS is the application of the sinusoidal voltage and measurement of the sinusoidal current response at a series of frequency points.

In the case of the piezoelectric actuator having the ac voltage applied to it, it generates stress varying sinusoidally in time due to the inverse piezoelectric effect. Depending on the frequency the resulting strain may be amplified due to the mechanical resonance. Such an amplified strain causes the generation of charge due to the direct piezoelectric effect. The magnitude of that charge is proportional to the magnitude of the strain and it may be measured electrically, as the charge $Q(t)$ sinusoidally varying in time with a radial frequency ω is equal to:

$$Q(t) = \int I(t)dt = \int I_0 \cos(\omega t)dt = \frac{I_0}{\omega} \sin(\omega t) = \frac{|Y| U_0}{\omega} \sin(\omega t), \quad (3)$$

where $I(t)$ is the current; I_0 is the magnitude of the current; Y is the measured admittance; U_0 is the magnitude of the applied voltage. Therefore, plotting $\frac{|Y|}{\omega} U_0$ it may be obtained a plot which will enable to visualise the mechanical resonances of the piezoelectric actuator. In practice, the measured admittance is also influenced by the displacement current of the piezoelectric actuator but in most cases its influence may be neglected.

The source of x and y signals are Analog Devices AD5546 16-bit DACs. The scan field arithmetic is implemented using 12-bit AD7398 DACs working as digital potentiometers. The Scan Field Controller is also equipped with multiple auxiliary 12- and 16-bit DAC channels helpful in performing additional functions, such as sample biasing or spectroscopy measurements. All analogue outputs operate within a ± 10 V range.

Using an 18-bit ADC module described in the following section and the procedure of noise floor measurements, we determined the performance of DACs. Main X, Y outputs achieve up to -100 dB_{FS} noise during the dynamic operation, while the static noise of polarization outputs is no higher than the ADC module's input noise with a linearity error equal to 0.75% in the full range.

2.3. Analogue-to-digital converter (ADC) module

The whole analogue signal acquisition in the ARMScope controller is performed using an ADC module based on the Linear Technologies LTC2348-18 low-noise, 8-channel, 18-bit successive approximation ADC [2] controlled by the circuitry implemented in the FPGA (Xilinx SPARTAN-3). The ADC is capable of up to 200 kcps simultaneous sampling of each of 8 channels or up to 1 Msps sampling of a single channel. The ADC module has 8 differential voltage inputs with a ± 10 V range. As the regular SPM measurements usually do not require such a fast sampling rate, the ADC module uses hardware-implemented oversampling and averaging up to 128 samples to improve the resolution.

The performance of the ADC module was evaluated by measuring the noise floor which limits the small-signal resolution. The results are shown in Fig. 4. Without averaging the standard deviation of samples is less than 1.5 bits which corresponds to -105 dB_{FS} (magnitude referenced to the full-scale voltage) noise floor and $165 \mu\text{V}$ resolution. The use of averaging improves these parameters up to -126 dB_{FS} and $12.5 \mu\text{V}$, respectively.

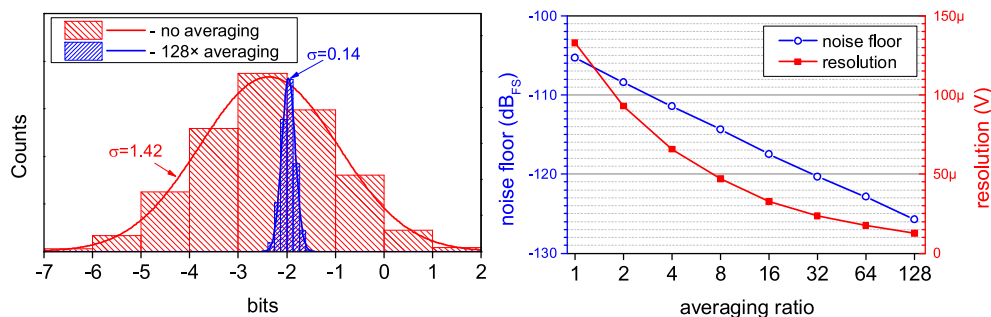


Fig. 4. The ADC module performance evaluated basing on the analysis of 2^{16} samples: histograms and Gaussian distribution curves using 128x and no averaging expressed in bits of resolution of the 18-bit ADC (left), noise floor expressed relative to the full scale voltage and a resulting voltage resolution of the ADC module at a ± 10 V range (right).

2.4. PID controller

A PID regulator is the most crucial part of SPM microscopes. The PID regulator is a part of the closed-loop path in the microscope, between the scanning probe tip and Z-axis actuator electronics, and is regulating interaction magnitude between the probe tip and a sample (z-axis) to keep constant deflection or amplitude vibration of the cantilever in the case of the AFM or current signal in the case of the STM, regardless of changes in the surface height during scan.

The PID controller consists of an error preamplifier, proportional, integral, derivative paths and a signal adder. A schematic of PID controller is shown in Fig. 5. The regulator compares the output signal from the scanning head with a set-point signal, giving as a result an error signal. The error signal passes through three connected in parallel PID paths performing mathematical operations. In the end, the signals from PID blocks are summed up giving the PID output signal, which controls movement of the piezo-actuator by the HV amplifier in such a way as to bring the error signal down to a possibly smallest value.

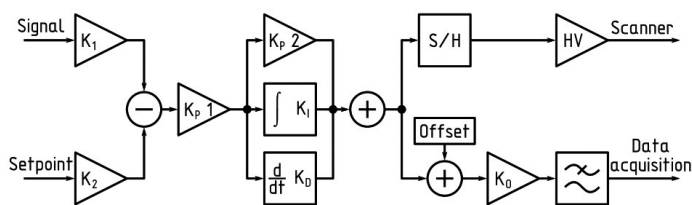


Fig. 5. A block diagram of PID controller.

To ensure an appropriate dynamics of the PID controller, its user needs to adjust PID parameters, such as a gain of proportional stage and time constants of both integral and derivative stages. The dynamics of the system must be tuned up in a given probe assembly-sample setup in order to obtain the fastest possible regulation time with stable operation during scanning.

In the ARMScope described here the SPM analogue PID controller with a continuous output was used – the whole signal path from input to output is made using linear amplifiers, the signal not being converted to the digital form. The use of this type of regulator ensures a very big dynamics of regulation, especially desired while approaching the sample, and provides excellent stability of operation during the scan. To ensure fast and user-friendly tuning of the PID parameters, 20 kΩ digital potentiometers were used. The digital potentiometers are controlled by an 8-bit microcontroller with USB interface to communicate with a PC. The USB interface is galvanically isolated from PC, using an ADUM1402 IC to reduce crosstalk of electrical noise from the computer. The use of 10-bit digital potentiometers enables to tune gains and time constants with a high accuracy. Our PID controller can be described by (3) and a time constant is described by (4):

$$G(s) = k_{P1} \left(k_{P2} + \frac{1}{T_I s} + k_D T_D s \right), \quad (4)$$

$$U(t) = k_{P1} \left(k_{P2} e(t) + \frac{\int_0^t e(t) dt}{T_I} + k_D T_D \frac{de(t)}{dt} \right). \quad (5)$$

Possible settings controlled by the digital potentiometers are grouped in Table 1. The PID regulator described here is an independent PCB connected to the ARMScope controller bus only to supply lines. The digital interface is connected directly to PC.

Table 1. Digitally set parameters of PID Controller.

Parameter	Unit	Minimum value	Maximum value
K_{P1}	V/V	0.0476	1
K_{P2}	V/V	0.0536	0.9464
T_I for STM ($C_I = 68$ nF)	s	0.0112	1.50722
T_I for AFM ($C_I = 100$ nF)	s	0.0165	2.2165
K_D	V/V	0.0536	0.9464
T_D ($C_I = 10$ nF)	s	0.0015	0.2015

An example of PID open-loop output function as a result of intentionally modulated input is presented in Fig. 6.

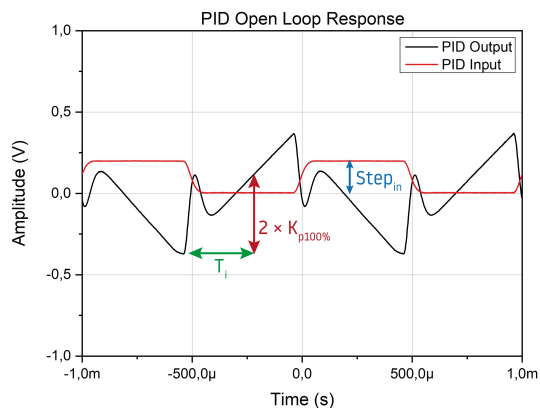


Fig. 6. The step-response open-loop output of PID regulator with an integral branch gain set to 100%, a proportional branch gain set to 100% and a derivative branch gain set to 75%. Integrator and differentiator circuits have capacitances $C_I = C_D = 10$ nF. PID regulator parameters that can be estimated: $T_i = 300$ μ s, $K_{P100\%} = 1$ V/V.

2.5. High-voltage driver section

Scanning Probe Microscope uses piezo-elements to position the micro-cantilever above the sample with a high accuracy and to control the magnitude of interactions (*e.g.* the force applied between the tip and the sample or the tunnelling current amplitude). The home-made ARMScope SPM is equipped with the custom-made piezo-tube-based scanner.

To apply in the STM system, our piezo-tube scanner has the maximum scan area of 100 nm \times 100 nm. Scans with a subatomic resolution require a high speed of movement. Our solution achieved up to 85 lines per second, which is enough for imaging graphene membranes (Fig. 7).

Our standard AFM scanner provides a displacement in the area up to 15 μ m \times 15 μ m driven with a bipolar ± 150 V. For driving such an actuator, we designed a compact high-voltage amplifier, which is part of ARMScope controller. This module has the form of an add-on board mounted onto the PID regulator circuit in order to enhance the noise performance of the Z-axis electrical control path. The module consists of three independent functional blocks to control X, Y and Z axes. Furthermore, all channels have a switched gain of 1 V/V and 10 V/V, which enables to enhance resolution of topography scans onto sub-nanometre details or to increase the scan area.

For driving the scanner with the maximum speed and maximum piezo-element displacement, the stage has to have a slew rate of fractions of volts per microsecond to avoid unwanted harmonic distortions. The designed output stage is based on Apex PA340 power operational amplifiers which have $SR = 32 \text{ V}/\mu\text{s}$, which more than satisfies the minimum requirements. Also, the output current capability of over 100 mA enables to smoothly drive the piezoelectric tube scanner with a high resolution. The noise of HV section is equal to $384 \mu\text{V}_{\text{RMS}}$ in a 10 kHz bandwidth.

On the other hand, sometimes the piezo-tube-based scanner has too small a scanning range for some AFM applications. For that reason, the system is designed in a very versatile way, which enables to assemble the AFM head with piezo-stages or flexural tables and connect external unipolar high-voltage amplifiers. In the setup described here, integration of a commercially available flexural stage Nano-MET3 (by courtesy of MadCityLabs Inc.) with a dedicated external HV driver is possible. This extends the scan area up to $100 \mu\text{m} \times 100 \mu\text{m}$ with scan speeds of a few lines per second.

The unipolar HV section for driving piezo-stacks that require unipolar driving voltages in a range of $-10 \text{ V} \div +125 \text{ V}$ can be connected to the system controller via external connectors and a bypassing bipolar unit. We have developed a compatible HV driver basing on Apex PA78 power operational amplifiers with outstanding performance parameters, when compared to the requirements for driving nano-positioning piezo-stages. The inputs driving X, Y signals, which are within a range of $-10 \text{ V} \div +10 \text{ V}$, cannot be straightforwardly amplified in the unipolar driving way, since the output driving voltage should be half of the maximum amplitude when none or 0V input signal is provided. Therefore, the driving signal has to be conditioned and to have an offset added to it in order to fit into the required voltage range.

3. Examples of measurements

The SPM system described in this paper is able to perform measurements working in various modes. Some examples of such measurements are presented below.

3.1. STM

Atomic-scale resolution tunnelling current images of HOPG (*Highly Oriented Pyrolytic Graphite*) sample scans obtained with STM are presented in Fig. 7. In Fig. 7 (left) there is a scan area of $12 \times 12 \text{ nm}^2$. Due to the visible edge between graphene layers, different arrange-

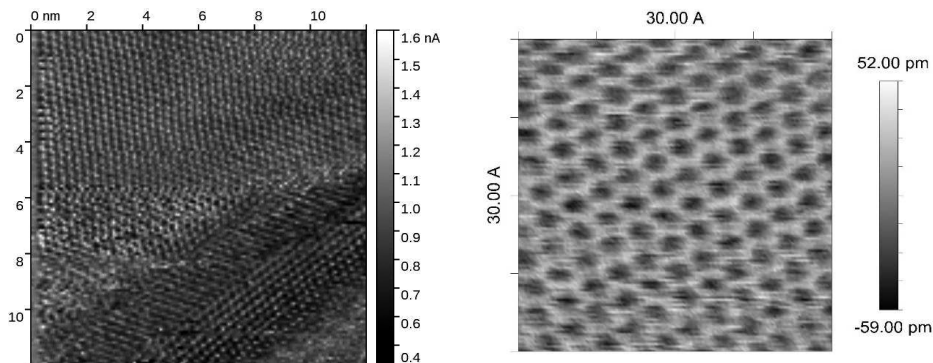


Fig. 7. HOPG STM tunnelling current image with a visible edge between graphene layers (left), STM tunnelling current image of an atom structure of HOPG (right).

ments of atoms can be observed. Atoms in the upper part of the image are packed in parallel to the top edge of the image, while atoms in the lower part of Fig. 7 are arranged in an angle in relation to the bottom edge of the image. In Fig. 7 (right), a clear atom structure of HOPG obtained in ambient air is presented.

3.2. Topography measurements

The contact mode is the basic mode of AFM operation, where the tip is in continuous contact with the sample. The cantilever deflection is set by the user and is related to the contact force between the tip and the surface. Therefore, soft cantilevers ($k < 1$ N/m) are preferred to avoid unintentional sample damage during measurement. The cantilever deflection is controlled by PID controller while the probe is moving above the scanned sample surface. In Fig. 8 images of HOPG and 6H-SiC (SiC/1.5 manufactured by TipsNano) samples are shown.

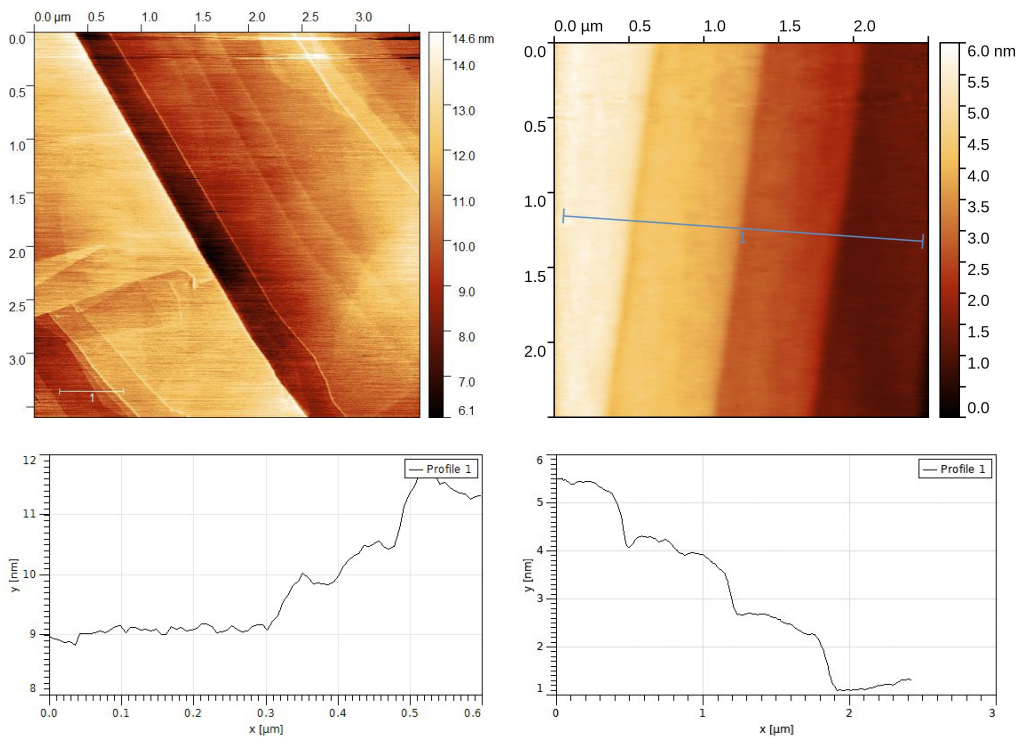


Fig. 8. An AFM image of HOPG sample obtained with Cont-PPP probes. A topography image of HOPG, scan area $3.6 \times 3.6 \mu\text{m}^2$ (top left), cross-section marked (top left) as "1"; atomic steps can be distinguished (bottom left). A topography image of silicon carbide, scan area $2.5 \times 2.5 \mu\text{m}^2$ (top right), cross-section marked (top right) as "1"; structural steps can be distinguished (bottom right).

3.3. Multi-resonance KPFM

Multi-resonance KPFM enables to separate mechanical actuation frequency and electrostatic carrier frequency in the non-contact mode. In the setup described here, it is possible to control cantilever oscillation in the second eigen-mode while measuring and controlling electrostatic

interactions at the first eigen-mode of the cantilever. The quality of the images was assessed through application of information capacity, which in the case described here equalled $ICC = 692 \text{ B}/\mu\text{m}$ [13].

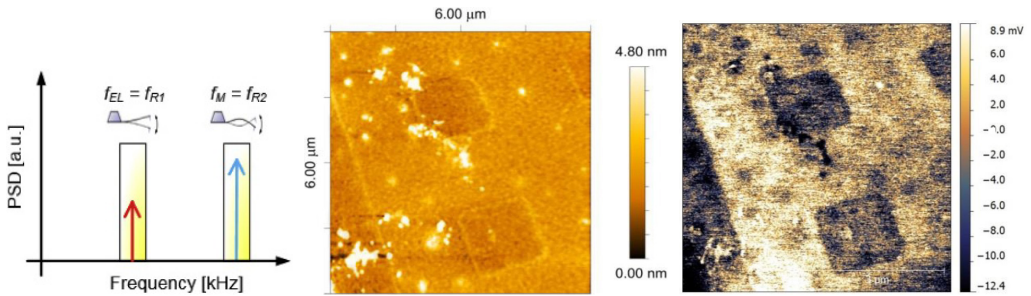


Fig. 9. Images of topography (middle) and CPD (*contact potential difference*) (right) of a microprinted SAM monolayer (11-MUA) on a gold surface in Multi-resonance KPFM (left). Images were obtained using a PPP-EFM cantilever from Nanosensors ($f = 75 \text{ kHz}$, $k = 3 \text{ N/m}$, first eigen-mode $Q = 150$, second eigen-mode $Q = 450$) [19].

Acknowledgements

The authors would like to express their gratitude to all the students and PhD students who have supported the development of the described setup over the past years for their work on ARMScope AFM prototype, especially to Michał Zielony, Maciej Słociński and Dr Grzegorz Józwiak.

The development of the PID controller, HV electronics and Scan field controller was carried out within the National Science Center (NCN) Preludium 11 Grant (Grant No. 2016/21/N/ST7/02275).

The STM examinations were supported by the Wrocław University of Science and Technology (WrUST) statutory grant.

References

- [1] Binnig, G., Quate, C.F. (1986). Atomic Force Microscope. *Phys. Rev. Lett.*, 56, 930–933.
- [2] Park NX20 Brochure: https://www.parksystems.co.jp/images/media/brochures/nx20/park_NX20151020E16AB.pdf (Jul 2019).
- [3] Rode, S., Stark, R., Lübke, J., Tröger, L., Schütte, J., Umeda, K., Kühnle, A. (2011). Modification of a commercial atomic force microscopy for low-noise, high-resolution frequency-modulation imaging in liquid environment. *Review of Scientific Instruments*, 82(7).
- [4] Yacoot, A., Koenders, L. (2011). Recent developments in dimensional nanometrology using AFMs. *Measurement Science and Technology*, 22(12).
- [5] Danzebrink, H.U., Koenders, L., Wilkening, G., Yacoot, A., Kunzmann, H. (2006). Advances in scanning force microscopy for dimensional metrology. *CIRP Annals – Manufacturing Technology*, 55(2).
- [6] Hohlbauch, S.V. (2018). Video Rate Atomic Force Microscopy of Biological Samples. *Biophys. J.*, 114.

- [7] Ahmad, A., Ivanov, T., Angelov, T., Rangelow, I. (2015). Fast atomic force microscopy with self-transduced, self-sensing cantilever. *J. Micro/Nanolith. MEMS MOEMS*, 14(3).
- [8] Ando, T. (2012). High-speed atomic force microscopy coming of age. *Nanotechnology*, 23(6).
- [9] Szyszka, A., Obłąk, M., Szymański, T., Wośko, M., Dawidowski, W., Paszkiewicz, R. (2016). Scanning capacitance microscopy characterization of AlInBV epitaxial layers. *Mater. Sci. Pol.*, 34, 845–850.
- [10] Dufrêne, Y.F., Ando, T., Garcia, R., Alsteens, D., Martinez-Martin, D., Engel, A., Müller, D.J. (2017). Imaging modes of atomic force microscopy for application in molecular and cell biology. *Nature Publishing Group*, 12.
- [11] Alessandrini, A., Facci, P. (2005). AFM: A versatile tool in biophysics. *Measurement Science and Technology*, 16(6).
- [12] Janshoff, Neitzert, Oberdörfer, Fuchs (2000). Force Spectroscopy of Molecular Systems-Single Molecule Spectroscopy of Polymers and Biomolecules. *Angewandte Chemie*, 39(18), 3212–3237.
- [13] RHK product catalog: <https://www.rhk-tech.com/r9plus/>.
- [14] Oxford Instruments catalog: <https://afm.oxinst.com/products/mfp-3d-afm-systems/>.
- [15] Kopiec, D., Józwiak, G., Moczala, M., Sierakowski, A., Gotszalk, T. (2018). Multifrequency Kelvin probe force microscopy on self assembled molecular layers and quantitative assessment of images' quality. *Ultramicroscopy*, 194, 100–107.
- [16] Biczysko, P., Dzierka, A., Józwiak, G., Rudek, M., Gotszalk, T., Janus, P., Grabiec, P., Rangelow, I.W. (2018). Contact atomic force microscopy using piezoresistive cantilevers in load force modulation mode. *Ultramicroscopy*, 184(2018), 199–208.
- [17] Gajewski, K., Kunicki, P., Sierakowski, A., Szymański, W., Kaczorowski, W., Niedzielski, P., Gotszalk, T. (2019). High-resolution, spatially-resolved surface potential investigations of high-strength metallurgical graphene using scanning tunnelling potentiometry. *Microelectronic Engineering*, 212, 1–8.
- [18] Świadkowski, B., Majstrzyk, W., et al. (2019). Near zero contact force atomic microscopy investigations using active electromagnetic cantilevers. submitted to *Ultramicroscopy*.
- [19] Kopiec, D., Józwiak, G., Moczala, M., Sierakowski, A., Gotszalk, T. (2018). Multifrequency Kelvin probe microscopy on self assembled molecular layers and quantitative assessment of images' quality. Reprinted from *Ultramicroscopy*, 194, 100–107.